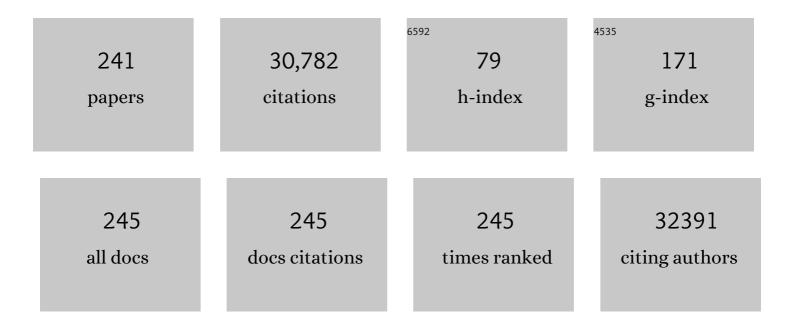
Christopher B Murray

List of Publications by Year in descending order

Source: https://exaly.com/author-pdf/4067039/publications.pdf Version: 2024-02-01



#	Article	IF	CITATIONS
1	Structural diversity in binary nanoparticle superlattices. Nature, 2006, 439, 55-59.	13.7	1,956
2	PbSe Nanocrystal Solids for n- and p-Channel Thin Film Field-Effect Transistors. Science, 2005, 310, 86-89.	6.0	1,551
3	Designing PbSe Nanowires and Nanorings through Oriented Attachment of Nanoparticles. Journal of the American Chemical Society, 2005, 127, 7140-7147.	6.6	1,195
4	Control of Metal Nanocrystal Size Reveals Metal-Support Interface Role for Ceria Catalysts. Science, 2013, 341, 771-773.	6.0	1,142
5	Prospects of Nanoscience with Nanocrystals. ACS Nano, 2015, 9, 1012-1057.	7.3	1,005
6	Using Binary Surfactant Mixtures To Simultaneously Improve the Dimensional Tunability and Monodispersity in the Seeded Growth of Gold Nanorods. Nano Letters, 2013, 13, 765-771.	4.5	910
7	Nonaqueous Synthesis of TiO ₂ Nanocrystals Using TiF ₄ to Engineer Morphology, Oxygen Vacancy Concentration, and Photocatalytic Activity. Journal of the American Chemical Society, 2012, 134, 6751-6761.	6.6	854
8	A Generalized Ligand-Exchange Strategy Enabling Sequential Surface Functionalization of Colloidal Nanocrystals. Journal of the American Chemical Society, 2011, 133, 998-1006.	6.6	770
9	Binary nanocrystal superlattice membranes self-assembled at the liquid–air interface. Nature, 2010, 466, 474-477.	13.7	758
10	Improved Size-Tunable Synthesis of Monodisperse Gold Nanorods through the Use of Aromatic Additives. ACS Nano, 2012, 6, 2804-2817.	7.3	749
11	Cluster-Assembled Materials. ACS Nano, 2009, 3, 244-255.	7.3	598
12	Quasicrystalline order in self-assembled binary nanoparticle superlattices. Nature, 2009, 461, 964-967.	13.7	551
13	Synergism in binary nanocrystal superlattices leads to enhanced p-type conductivity in self-assembled PbTe/Ag2Te thin films. Nature Materials, 2007, 6, 115-121.	13.3	498
14	Charge transport in strongly coupled quantum dot solids. Nature Nanotechnology, 2015, 10, 1013-1026.	15.6	473
15	Structural Characterization of Self-Assembled Multifunctional Binary Nanoparticle Superlattices. Journal of the American Chemical Society, 2006, 128, 3620-3637.	6.6	452
16	Synthesis of Monodisperse Nanoparticles of Barium Titanate:Â Toward a Generalized Strategy of Oxide Nanoparticle Synthesis. Journal of the American Chemical Society, 2001, 123, 12085-12086.	6.6	450
17	Morphologically controlled synthesis of colloidal upconversion nanophosphors and their shape-directed self-assembly. Proceedings of the National Academy of Sciences of the United States of America, 2010, 107, 22430-22435.	3.3	416
18	Platinum nanocrystals selectively shaped using facet-specific peptide sequences. Nature Chemistry, 2011, 3, 393-399.	6.6	404

#	Article	IF	CITATIONS
19	Magnetic, Electronic, and Structural Characterization of Nonstoichiometric Iron Oxides at the Nanoscale. Journal of the American Chemical Society, 2004, 126, 14583-14599.	6.6	393
20	Solution-Phase Synthesis of Titanium Dioxide Nanoparticles and Nanocrystals. Chemical Reviews, 2014, 114, 9319-9345.	23.0	343
21	Synthesis and Electrocatalytic Properties of Cubic Mnâ^'Pt Nanocrystals (Nanocubes). Journal of the American Chemical Society, 2010, 132, 7568-7569.	6.6	341
22	Bandlike Transport in Strongly Coupled and Doped Quantum Dot Solids: A Route to High-Performance Thin-Film Electronics. Nano Letters, 2012, 12, 2631-2638.	4.5	340
23	Dipoleâ^'Dipole Interactions in Nanoparticle Superlattices. Nano Letters, 2007, 7, 1213-1219.	4.5	316
24	Self-Assembly of PbTe Quantum Dots into Nanocrystal Superlattices and Glassy Films. Journal of the American Chemical Society, 2006, 128, 3248-3255.	6.6	310
25	Thiocyanate-Capped Nanocrystal Colloids: Vibrational Reporter of Surface Chemistry and Solution-Based Route to Enhanced Coupling in Nanocrystal Solids. Journal of the American Chemical Society, 2011, 133, 15753-15761.	6.6	309
26	CdSe and CdSe/CdS Nanorod Solids. Journal of the American Chemical Society, 2004, 126, 12984-12988.	6.6	279
27	Competition of shape and interaction patchiness for self-assembling nanoplates. Nature Chemistry, 2013, 5, 466-473.	6.6	278
28	Synthesis, Shape Control, and Methanol Electro-oxidation Properties of Pt–Zn Alloy and Pt ₃ Zn Intermetallic Nanocrystals. ACS Nano, 2012, 6, 5642-5647.	7.3	273
29	Metal-Enhanced Upconversion Luminescence Tunable through Metal Nanoparticle–Nanophosphor Separation. ACS Nano, 2012, 6, 8758-8766.	7.3	262
30	Exploiting the colloidal nanocrystal library to construct electronic devices. Science, 2016, 352, 205-208.	6.0	234
31	Enhanced Thermopower via Carrier Energy Filtering in Solution-Processable Pt–Sb ₂ Te ₃ Nanocomposites. Nano Letters, 2011, 11, 2841-2844.	4.5	230
32	The State of Nanoparticle-Based Nanoscience and Biotechnology: Progress, Promises, and Challenges. ACS Nano, 2012, 6, 8468-8483.	7.3	211
33	Stoichiometric Control of Lead Chalcogenide Nanocrystal Solids to Enhance Their Electronic and Optoelectronic Device Performance. ACS Nano, 2013, 7, 2413-2421.	7.3	210
34	Synthesis of Monodisperse PbSe Nanorods: A Case for Oriented Attachment. Journal of the American Chemical Society, 2010, 132, 3909-3913.	6.6	209
35	Efficient Removal of Organic Ligands from Supported Nanocrystals by Fast Thermal Annealing Enables Catalytic Studies on Well-Defined Active Phases. Journal of the American Chemical Society, 2015, 137, 6906-6911.	6.6	208
36	Seeded Growth of Monodisperse Gold Nanorods Using Bromide-Free Surfactant Mixtures. Nano Letters, 2013, 13, 2163-2171.	4.5	200

#	Article	IF	CITATIONS
37	Plasmonic Enhancement of Nanophosphor Upconversion Luminescence in Au Nanohole Arrays. ACS Nano, 2013, 7, 7186-7192.	7.3	199
38	Bimetallic synergy in cobalt–palladium nanocatalysts for CO oxidation. Nature Catalysis, 2019, 2, 78-85.	16.1	195
39	Shape-Dependent Plasmonic Response and Directed Self-Assembly in a New Semiconductor Building Block, Indium-Doped Cadmium Oxide (ICO). Nano Letters, 2013, 13, 2857-2863.	4.5	182
40	Design of Pt–Pd Binary Superlattices Exploiting Shape Effects and Synergistic Effects for Oxygen Reduction Reactions. Journal of the American Chemical Society, 2013, 135, 42-45.	6.6	180
41	Emergence of complexity in hierarchically organized chiral particles. Science, 2020, 368, 642-648.	6.0	179
42	Highly Active Pt ₃ Pb and Core–Shell Pt ₃ Pb–Pt Electrocatalysts for Formic Acid Oxidation. ACS Nano, 2012, 6, 2818-2825.	7.3	177
43	Designing High-Performance PbS and PbSe Nanocrystal Electronic Devices through Stepwise, Post-Synthesis, Colloidal Atomic Layer Deposition. Nano Letters, 2014, 14, 1559-1566.	4.5	176
44	Substitutional doping in nanocrystal superlattices. Nature, 2015, 524, 450-453.	13.7	174
45	Thiocyanate-Capped PbS Nanocubes: Ambipolar Transport Enables Quantum Dot Based Circuits on a Flexible Substrate. Nano Letters, 2011, 11, 4764-4767.	4.5	171
46	Monodisperse Core/Shell Ni/FePt Nanoparticles and Their Conversion to Ni/Pt to Catalyze Oxygen Reduction. Journal of the American Chemical Society, 2014, 136, 15921-15924.	6.6	165
47	Shape-Controlled Synthesis of Pt Nanocrystals: The Role of Metal Carbonyls. ACS Nano, 2013, 7, 645-653.	7.3	162
48	Visualizing non-equilibrium lithiation of spinel oxide via in situ transmission electron microscopy. Nature Communications, 2016, 7, 11441.	5.8	162
49	Two-Dimensional Binary and Ternary Nanocrystal Superlattices: The Case of Monolayers and Bilayers. Nano Letters, 2011, 11, 1804-1809.	4.5	159
50	Polymorphism in AB13Nanoparticle Superlattices:Â An Example of Semiconductorâ^'Metal Metamaterials. Journal of the American Chemical Society, 2005, 127, 8741-8747.	6.6	158
51	Doubling the Efficiency of Third Harmonic Generation by Positioning ITO Nanocrystals into the Hot-Spot of Plasmonic Gap-Antennas. Nano Letters, 2014, 14, 2867-2872.	4.5	155
52	Photocatalytic Hydrogen Evolution from Substoichiometric Colloidal WO _{3–<i>x</i>} Nanowires. ACS Energy Letters, 2018, 3, 1904-1910.	8.8	145
53	Collective Dipolar Interactions in Self-Assembled Magnetic Binary Nanocrystal Superlattice Membranes. Nano Letters, 2010, 10, 5103-5108.	4.5	143
54	One-step green synthesis of gold and silver nanoparticles with ascorbic acid and their versatile surface post-functionalization. RSC Advances, 2016, 6, 33092-33100.	1.7	141

#	Article	IF	CITATIONS
55	Synthesis and X-ray Characterization of Cobalt Phosphide (Co ₂ P) Nanorods for the Oxygen Reduction Reaction. ACS Nano, 2015, 9, 8108-8115.	7.3	132
56	Plasmon-Enhanced Upconversion Luminescence in Single Nanophosphor–Nanorod Heterodimers Formed through Template-Assisted Self-Assembly. ACS Nano, 2014, 8, 9482-9491.	7.3	127
57	Tunable Plasmonic Coupling in Self-Assembled Binary Nanocrystal Superlattices Studied by Correlated Optical Microspectrophotometry and Electron Microscopy. Nano Letters, 2013, 13, 1291-1297.	4.5	125
58	Mechanisms for High Selectivity in the Hydrodeoxygenation of 5-Hydroxymethylfurfural over PtCo Nanocrystals. ACS Catalysis, 2016, 6, 4095-4104.	5.5	124
59	Synthesis of Colloidal PbSe/PbS Coreâ^'Shell Nanowires and PbS/Au Nanowireâ~'Nanocrystal Heterostructures. Journal of Physical Chemistry C, 2007, 111, 14049-14054.	1.5	122
60	Engineering Catalytic Contacts and Thermal Stability: Gold/Iron Oxide Binary Nanocrystal Superlattices for CO Oxidation. Journal of the American Chemical Society, 2013, 135, 1499-1505.	6.6	122
61	Methane Oxidation on Pd@ZrO ₂ /Si–Al ₂ O ₃ Is Enhanced by Surface Reduction of ZrO ₂ . ACS Catalysis, 2014, 4, 3902-3909.	5.5	119
62	Expanding the Spectral Tunability of Plasmonic Resonances in Doped Metal-Oxide Nanocrystals through Cooperative Cation–Anion Codoping. Journal of the American Chemical Society, 2014, 136, 11680-11686.	6.6	119
63	Designing Tripodal and Triangular Gadolinium Oxide Nanoplates and Self-Assembled Nanofibrils as Potential Multimodal Bioimaging Probes. ACS Nano, 2013, 7, 2850-2859.	7.3	115
64	Quasicrystalline nanocrystal superlattice with partial matching rules. Nature Materials, 2017, 16, 214-219.	13.3	114
65	In vivo multiple color lymphatic imaging using upconverting nanocrystals. Journal of Materials Chemistry, 2009, 19, 6481.	6.7	112
66	Solution-Processed Phase-Change VO ₂ Metamaterials from Colloidal Vanadium Oxide (VO _{<i>x</i>}) Nanocrystals. ACS Nano, 2014, 8, 797-806.	7.3	112
67	Binary and Ternary Superlattices Self-Assembled from Colloidal Nanodisks and Nanorods. Journal of the American Chemical Society, 2015, 137, 6662-6669.	6.6	110
68	Engineering titania nanostructure to tune and improve its photocatalytic activity. Proceedings of the National Academy of Sciences of the United States of America, 2016, 113, 3966-3971.	3.3	106
69	Heterogeneous Catalysts Need Not Be so "Heterogeneous― Monodisperse Pt Nanocrystals by Combining Shape-Controlled Synthesis and Purification by Colloidal Recrystallization. Journal of the American Chemical Society, 2013, 135, 2741-2747.	6.6	105
70	Shape Alloys of Nanorods and Nanospheres from Self-Assembly. Nano Letters, 2013, 13, 4980-4988.	4.5	104
71	Properties of CdSe nanocrystal dispersions in the dilute regime: Structure and interparticle interactions. Physical Review B, 1998, 58, 7850-7863.	1.1	101
72	Engineering Charge Injection and Charge Transport for High Performance PbSe Nanocrystal Thin Film Devices and Circuits. Nano Letters, 2014, 14, 6210-6216.	4.5	100

#	Article	IF	CITATIONS
73	Base metal-Pt alloys: A general route to high selectivity and stability in the production of biofuels from HMF. Applied Catalysis B: Environmental, 2016, 199, 439-446.	10.8	100
74	Dendritic upconverting nanoparticles enable in vivo multiphoton microscopy with low-power continuous wave sources. Proceedings of the National Academy of Sciences of the United States of America, 2012, 109, 20826-20831.	3.3	88
75	Chemically Tailored Dielectric-to-Metal Transition for the Design of Metamaterials from Nanoimprinted Colloidal Nanocrystals. Nano Letters, 2013, 13, 350-357.	4.5	87
76	Studies of Liquid Crystalline Self-Assembly of GdF ₃ Nanoplates by In-Plane, Out-of-Plane SAXS. ACS Nano, 2011, 5, 8322-8330.	7.3	86
77	Enhanced Charge Transfer Kinetics of CdSe Quantum Dot-Sensitized Solar Cell by Inorganic Ligand Exchange Treatments. ACS Applied Materials & Interfaces, 2014, 6, 3721-3728.	4.0	86
78	Bistable Magnetoresistance Switching in Exchange-Coupled CoFe ₂ O ₄ –Fe ₃ O ₄ Binary Nanocrystal Superlattices by Self-Assembly and Thermal Annealing. ACS Nano, 2013, 7, 1478-1486.	7.3	85
79	Polymorphism in Self-Assembled AB ₆ Binary Nanocrystal Superlattices. Journal of the American Chemical Society, 2011, 133, 2613-2620.	6.6	84
80	Unraveling the surface state and composition of highly selective nanocrystalline Ni–Cu alloy catalysts for hydrodeoxygenation of HMF. Catalysis Science and Technology, 2017, 7, 1735-1743.	2.1	82
81	Interplay between spherical confinement and particle shape on the self-assembly of rounded cubes. Nature Communications, 2018, 9, 2228.	5.8	81
82	Multiscale Periodic Assembly of Striped Nanocrystal Superlattice Films on a Liquid Surface. Nano Letters, 2011, 11, 841-846.	4.5	79
83	Plasmon Resonances in Self-Assembled Two-Dimensional Au Nanocrystal Metamolecules. ACS Nano, 2017, 11, 2917-2927.	7.3	78
84	Generalized Synthetic Strategy for Transition-Metal-Doped Brookite-Phase TiO ₂ Nanorods. Journal of the American Chemical Society, 2019, 141, 16548-16552.	6.6	78
85	Shape-Directed Binary Assembly of Anisotropic Nanoplates: A Nanocrystal Puzzle with Shape-Complementary Building Blocks. Nano Letters, 2013, 13, 2952-2956.	4.5	76
86	High-strength magnetically switchable plasmonic nanorods assembled from a binary nanocrystal mixture. Nature Nanotechnology, 2017, 12, 228-232.	15.6	75
87	Plasmonic Optical and Chiroptical Response of Self-Assembled Au Nanorod Equilateral Trimers. ACS Nano, 2019, 13, 1617-1624.	7.3	75
88	Large-Area Nanoimprinted Colloidal Au Nanocrystal-Based Nanoantennas for Ultrathin Polarizing Plasmonic Metasurfaces. Nano Letters, 2015, 15, 5254-5260.	4.5	73
89	Crystalline, Shape, and Surface Anisotropy in Two Crystal Morphologies of Superparamagnetic Cobalt Nanoparticles by Ferromagnetic Resonance. Journal of Physical Chemistry B, 2001, 105, 7913-7919.	1.2	72
90	High-Temperature Photoluminescence of CdSe/CdS Core/Shell Nanoheterostructures. ACS Nano, 2014, 8, 6466-6474.	7.3	71

#	Article	IF	CITATIONS
91	Smectic Nanorod Superlattices Assembled on Liquid Subphases: Structure, Orientation, Defects, and Optical Polarization. Chemistry of Materials, 2015, 27, 2998-3008.	3.2	69
92	Advanced Architecture for Colloidal PbS Quantum Dot Solar Cells Exploiting a CdSe Quantum Dot Buffer Layer. ACS Nano, 2016, 10, 9267-9273.	7.3	69
93	Synthesis of 1,3-Diynes in the Purine, Pyrimidine, 1,3,5-Triazine and Acridine Series. Tetrahedron, 2000, 56, 1233-1245.	1.0	68
94	Comparison of HMF hydrodeoxygenation over different metal catalysts in a continuous flow reactor. Applied Catalysis A: General, 2015, 508, 86-93.	2.2	68
95	Favorable Core/Shell Interface within Co ₂ P/Pt Nanorods for Oxygen Reduction Electrocatalysis. Nano Letters, 2018, 18, 7870-7875.	4.5	68
96	A Technology Overview of the PowerChip Development Program. IEEE Transactions on Power Electronics, 2013, 28, 4182-4201.	5.4	67
97	Nanocrystal Size-Dependent Efficiency of Quantum Dot Sensitized Solar Cells in the Strongly Coupled CdSe Nanocrystals/TiO ₂ System. ACS Applied Materials & Interfaces, 2016, 8, 14692-14700.	4.0	66
98	A comparison of furfural hydrodeoxygenation over Pt-Co and Ni-Fe catalysts at high and low H2 pressures. Catalysis Today, 2018, 302, 73-79.	2.2	66
99	Seeded Growth of Metal-Doped Plasmonic Oxide Heterodimer Nanocrystals and Their Chemical Transformation. Journal of the American Chemical Society, 2014, 136, 5106-5115.	6.6	65
100	Lifetime, Mobility, and Diffusion of Photoexcited Carriers in Ligand-Exchanged Lead Selenide Nanocrystal Films Measured by Time-Resolved Terahertz Spectroscopy. ACS Nano, 2015, 9, 1820-1828.	7.3	61
101	Temperature-Tuning of Near-Infrared Monodisperse Quantum Dot Solids at 1.5 µm for Controllable Förster Energy Transfer. Nano Letters, 2008, 8, 2006-2011.	4.5	60
102	Gold Nanorod Translocations and Charge Measurement through Solid-State Nanopores. Nano Letters, 2014, 14, 5358-5364.	4.5	59
103	Report from the third workshop on future directions of solid-state chemistry: The status of solid-state chemistry and its impact in the physical sciences. Progress in Solid State Chemistry, 2008, 36, 1-133.	3.9	58
104	Synergistic Oxygen Evolving Activity of a TiO ₂ -Rich Reconstructed SrTiO ₃ (001) Surface. Journal of the American Chemical Society, 2015, 137, 2939-2947.	6.6	58
105	Probing the Fermi Energy Level and the Density of States Distribution in PbTe Nanocrystal (Quantum) Tj ETQq1 1	0,784314	rgBT /Overle
106	Low-Frequency (1/ <i>f</i>) Noise in Nanocrystal Field-Effect Transistors. ACS Nano, 2014, 8, 9664-9672.	7.3	55
107	Protein-directed self-assembly of a fullerene crystal. Nature Communications, 2016, 7, 11429.	5.8	55
108	Enhanced Thermal Stability and Magnetic Properties in NaCl-Type FePt–MnO Binary Nanocrystal Superlattices. Journal of the American Chemical Society, 2011, 133, 13296-13299.	6.6	54

#	Article	IF	CITATIONS
109	The H2 Pressure Dependence of Hydrodeoxygenation Selectivities for Furfural Over Pt/C Catalysts. Catalysis Letters, 2016, 146, 711-717.	1.4	54
110	General Synthetic Route to High-Quality Colloidal III–V Semiconductor Quantum Dots Based on Pnictogen Chlorides. Journal of the American Chemical Society, 2019, 141, 15145-15152.	6.6	54
111	Alignment, Electronic Properties, Doping, and On-Chip Growth of Colloidal PbSe Nanowires. Journal of Physical Chemistry C, 2007, 111, 13244-13249.	1.5	53
112	Systematic Electron Crystallographic Studies of Self-Assembled Binary Nanocrystal Superlattices. ACS Nano, 2010, 4, 2374-2381.	7.3	52
113	<i>In Situ</i> Repair of High-Performance, Flexible Nanocrystal Electronics for Large-Area Fabrication and Operation in Air. ACS Nano, 2013, 7, 8275-8283.	7.3	52
114	Ultrafast Electron Trapping at the Surface of Semiconductor Nanocrystals: Excitonic and Biexcitonic Processes. Journal of Physical Chemistry B, 2013, 117, 4412-4421.	1.2	52
115	Deposition of Waferâ€Scale Singleâ€Component and Binary Nanocrystal Superlattice Thin Films Via Dipâ€Coating. Advanced Materials, 2015, 27, 2846-2851.	11.1	52
116	Flexible, High-Speed CdSe Nanocrystal Integrated Circuits. Nano Letters, 2015, 15, 7155-7160.	4.5	52
117	Coherent Acoustic Phonons in Colloidal Semiconductor Nanocrystal Superlattices. ACS Nano, 2016, 10, 1163-1169.	7.3	52
118	Near-Infrared Absorption of Monodisperse Silver Telluride (Ag ₂ Te) Nanocrystals and Photoconductive Response of Their Self-Assembled Superlattices. Chemistry of Materials, 2011, 23, 4657-4659.	3.2	51
119	Dendron-Mediated Engineering of Interparticle Separation and Self-Assembly in Dendronized Gold Nanoparticles Superlattices. Journal of the American Chemical Society, 2015, 137, 10728-10734.	6.6	51
120	Effect of Ni particle size on the production of renewable methane from CO2 over Ni/CeO2 catalyst. Journal of Energy Chemistry, 2021, 61, 602-611.	7.1	51
121	Engineering Localized Surface Plasmon Interactions in Gold by Silicon Nanowire for Enhanced Heating and Photocatalysis. Nano Letters, 2017, 17, 1839-1845.	4.5	50
122	Tunable Optical Anisotropy of Seeded CdSe/CdS Nanorods. Journal of Physical Chemistry Letters, 2014, 5, 85-91.	2.1	49
123	A Study of Tetrahydrofurfuryl Alcohol to 1,5-Pentanediol Over Pt–WOx/C. Catalysis Letters, 2018, 148, 1047-1054.	1.4	49
124	Increased Carrier Mobility and Lifetime in CdSe Quantum Dot Thin Films through Surface Trap Passivation and Doping. Journal of Physical Chemistry Letters, 2015, 6, 4605-4609.	2.1	47
125	Quantifying "Softness―of Organic Coatings on Gold Nanoparticles Using Correlated Small-Angle X-ray and Neutron Scattering. Nano Letters, 2015, 15, 8008-8012.	4.5	47
126	Synthesis of N-Type Plasmonic Oxide Nanocrystals and the Optical and Electrical Characterization of their Transparent Conducting Films. Chemistry of Materials, 2014, 26, 4579-4588.	3.2	46

#	Article	IF	CITATIONS
127	Probing the Structure, Composition, and Spatial Distribution of Ligands on Gold Nanorods. Nano Letters, 2015, 15, 5730-5738.	4.5	46
128	Preparation and Self-Assembly of Dendronized Janus Fe ₃ O ₄ –Pt and Fe ₃ O ₄ –Au Heterodimers. ACS Nano, 2017, 11, 7958-7966.	7.3	46
129	Carrier Distribution and Dynamics of Nanocrystal Solids Doped with Artificial Atoms. Nano Letters, 2010, 10, 1842-1847.	4.5	45
130	Size- and Composition-Dependent Radio Frequency Magnetic Permeability of Iron Oxide Nanocrystals. ACS Nano, 2014, 8, 12323-12337.	7.3	44
131	Gaussian processes for autonomous data acquisition at large-scale synchrotron and neutron facilities. Nature Reviews Physics, 2021, 3, 685-697.	11.9	44
132	Watching Nanocrystals Grow. Science, 2009, 324, 1276-1277.	6.0	43
133	Solution-Based Stoichiometric Control over Charge Transport in Nanocrystalline CdSe Devices. ACS Nano, 2013, 7, 8760-8770.	7.3	43
134	Synthesis and Size-Selective Precipitation of Monodisperse Nonstoichiometric M _{<i>x</i>} Fe _{3–<i>x</i>} O ₄ (M = Mn, Co) Nanocrystals and Their DC and AC Magnetic Properties. Chemistry of Materials, 2016, 28, 480-489.	3.2	42
135	Binary icosahedral clusters of hard spheres in spherical confinement. Nature Physics, 2021, 17, 128-134.	6.5	42
136	Shape-Controlled Synthesis of Isotopic Yttrium-90-Labeled Rare Earth Fluoride Nanocrystals for Multimodal Imaging. ACS Nano, 2015, 9, 8718-8728.	7.3	41
137	Improved Models for Metallic Nanoparticle Cores from Atomic Pair Distribution Function (PDF) Analysis. Journal of Physical Chemistry C, 2018, 122, 29498-29506.	1.5	41
138	Air-Stable, Nanostructured Electronic and Plasmonic Materials from Solution-Processable, Silver Nanocrystal Building Blocks. ACS Nano, 2014, 8, 2746-2754.	7.3	40
139	Nanodisco Balls: Control over Surface <i>versus</i> Core Loading of Diagnostically Active Nanocrystals into Polymer Nanoparticles. ACS Nano, 2014, 8, 9143-9153.	7.3	40
140	Hierarchical Materials Design by Pattern Transfer Printing of Self-Assembled Binary Nanocrystal Superlattices. Nano Letters, 2017, 17, 1387-1394.	4.5	40
141	Design, Self-Assembly, and Switchable Wettability in Hydrophobic, Hydrophilic, and Janus Dendritic Ligand–Gold Nanoparticle Hybrid Materials. Chemistry of Materials, 2017, 29, 8737-8746.	3.2	40
142	Tuning the Electrocatalytic Oxygen Reduction Reaction Activity of Pt–Co Nanocrystals by Cobalt Concentration with Atomic-Scale Understanding. ACS Applied Materials & Interfaces, 2019, 11, 26789-26797.	4.0	40
143	Investigating the Phosphine Chemistry of Se Precursors for the Synthesis of PbSe Nanorods. Chemistry of Materials, 2011, 23, 1825-1829.	3.2	39
144	Fast Nanorod Diffusion through Entangled Polymer Melts. ACS Macro Letters, 2015, 4, 952-956.	2.3	39

#	Article	IF	CITATIONS
145	Three-Dimensional Self-Assembly of Chalcopyrite Copper Indium Diselenide Nanocrystals into Oriented Films. ACS Nano, 2013, 7, 4307-4315.	7.3	38
146	Magnetic anisotropy considerations in magnetic force microscopy studies of single superparamagnetic nanoparticles. Nanotechnology, 2012, 23, 495704.	1.3	36
147	Revealing particle growth mechanisms by combining high-surface-area catalysts made with monodisperse particles and electron microscopy conducted at atmospheric pressure. Journal of Catalysis, 2016, 337, 240-247.	3.1	36
148	Nanoimprinted Chiral Plasmonic Substrates with Three-Dimensional Nanostructures. Nano Letters, 2018, 18, 7389-7394.	4.5	36
149	Angular measurements of the dynein ring reveal a stepping mechanism dependent on a flexible stalk. Proceedings of the National Academy of Sciences of the United States of America, 2017, 114, E4564-E4573.	3.3	35
150	<i>Cluster-mining</i> : an approach for determining core structures of metallic nanoparticles from atomic pair distribution function data. Acta Crystallographica Section A: Foundations and Advances, 2020, 76, 24-31.	0.0	34
151	Effects of Post-Synthesis Processing on CdSe Nanocrystals and Their Solids: Correlation between Surface Chemistry and Optoelectronic Properties. Journal of Physical Chemistry C, 2014, 118, 27097-27105.	1.5	33
152	Selective p- and n-Doping of Colloidal PbSe Nanowires To Construct Electronic and Optoelectronic Devices. ACS Nano, 2015, 9, 7536-7544.	7.3	32
153	Ambipolar and Unipolar PbSe Nanowire Field-Effect Transistors. ACS Nano, 2011, 5, 3230-3236.	7.3	31
154	Supported platinum–zinc oxide core–shell nanoparticle catalysts for methanol steam reforming. Journal of Materials Chemistry A, 2014, 2, 19509-19514.	5.2	31
155	Mineralizer-Assisted Shape-Control of Rare Earth Oxide Nanoplates. Chemistry of Materials, 2014, 26, 6328-6332.	3.2	31
156	Spectrally-Resolved Dielectric Functions of Solution-Cast Quantum Dot Thin Films. Chemistry of Materials, 2015, 27, 6463-6469.	3.2	31
157	Rare-Earth Sulfide Nanocrystals from Wet Colloidal Synthesis: Tunable Compositions, Size-Dependent Light Absorption, and Sensitized Rare-Earth Luminescence. Journal of the American Chemical Society, 2021, 143, 3300-3305.	6.6	31
158	Electric Fields on Oxidized Silicon Surfaces: Static Polarization of PbSe Nanocrystalsâ€. Journal of Physical Chemistry A, 2004, 108, 7814-7819.	1.1	30
159	Nanocrystal Core Size and Shape Substitutional Doping and Underlying Crystalline Order in Nanocrystal Superlattices. ACS Nano, 2019, 13, 5712-5719.	7.3	30
160	Functionalizing molecular wires: a tunable class of α,ω-diphenyl-μ,ν-dicyano-oligoenes. Chemical Science, 2012, 3, 1007.	3.7	29
161	Interpreting the Energy-Dependent Anisotropy of Colloidal Nanorods Using Ensemble and Single-Particle Spectroscopy. Journal of Physical Chemistry C, 2013, 117, 23928-23937.	1.5	28
162	Gold nanorod length controls dispersion, local ordering, and optical absorption in polymer nanocomposite films. Soft Matter, 2014, 10, 3404-3413.	1.2	28

#	Article	IF	CITATIONS
163	Uniform Bimetallic Nanocrystals by High-Temperature Seed-Mediated Colloidal Synthesis and Their Catalytic Properties for Semiconducting Nanowire Growth. Chemistry of Materials, 2015, 27, 5833-5838.	3.2	27
164	Rapid Large-Scale Assembly and Pattern Transfer of One-Dimensional Gold Nanorod Superstructures. ACS Applied Materials & Interfaces, 2017, 9, 25513-25521.	4.0	27
165	Enhanced Energy Transfer in Quasiâ€Quaternary Nanocrystal Superlattices. Advanced Materials, 2014, 26, 2419-2423.	11.1	26
166	Bulk Metallic Glass-like Scattering Signal in Small Metallic Nanoparticles. ACS Nano, 2014, 8, 6163-6170.	7.3	26
167	Characterization of Shape and Monodispersity of Anisotropic Nanocrystals through Atomistic X-ray Scattering Simulation. Chemistry of Materials, 2015, 27, 2502-2506.	3.2	26
168	Gate-Induced Carrier Delocalization in Quantum Dot Field Effect Transistors. Nano Letters, 2014, 14, 5948-5952.	4.5	25
169	Plasmonicâ€Based Mechanochromic Microcapsules as Strain Sensors. Small, 2017, 13, 1701925.	5.2	25
170	Thermal and photochemical reactions of methanol on nanocrystalline anatase TiO ₂ thin films. Physical Chemistry Chemical Physics, 2015, 17, 17190-17201.	1.3	24
171	Shape-dependence of the thermal and photochemical reactions of methanol on nanocrystalline anatase TiO2. Surface Science, 2016, 654, 1-7.	0.8	24
172	Alignment of Nanoplates in Lamellar Diblock Copolymer Domains and the Effect of Particle Volume Fraction on Phase Behavior. ACS Macro Letters, 2018, 7, 1400-1407.	2.3	24
173	Air-Stable CuInSe ₂ Nanocrystal Transistors and Circuits <i>via</i> Post-Deposition Cation Exchange. ACS Nano, 2019, 13, 2324-2333.	7.3	24
174	Unusual Dinitrogen Binding and Electron Storage in Dinuclear Iron Complexes. Journal of the American Chemical Society, 2020, 142, 8147-8159.	6.6	24
175	Thermal and Photocatalytic Reactions of Methanol and Acetaldehyde on Pt-Modified Brookite TiO ₂ Nanorods. ACS Catalysis, 2018, 8, 11834-11846.	5.5	23
176	Microreactor Chemical Bath Deposition of Laterally Graded Cd _{1–<i>x</i>} Zn _{<i>x</i>} S Thin Films: A Route to High-Throughput Optimization for Photovoltaic Buffer Layers. Chemistry of Materials, 2013, 25, 297-306.	3.2	22
177	Polycatenar Ligand Control of the Synthesis and Self-Assembly of Colloidal Nanocrystals. Journal of the American Chemical Society, 2016, 138, 10508-10515.	6.6	22
178	Ultrafast Photoluminescence from the Core and the Shell in CdSe/CdS Dotâ€inâ€Rod Heterostructures. ChemPhysChem, 2016, 17, 759-765.	1.0	22
179	Phase Behavior of Grafted Polymer Nanocomposites from Field-Based Simulations. Macromolecules, 2019, 52, 5110-5121.	2.2	22
180	Dendrimer Ligand Directed Nanoplate Assembly. ACS Nano, 2019, 13, 14241-14251.	7.3	22

#	Article	IF	CITATIONS
181	Simultaneous Photonic and Excitonic Coupling in Spherical Quantum Dot Supercrystals. ACS Nano, 2020, 14, 13806-13815.	7.3	22
182	Improved Chemical and Colloidal Stability of Gold Nanoparticles through Dendron Capping. Langmuir, 2018, 34, 13333-13338.	1.6	21
183	A Characterization Study of Reactive Sites in ALD-Synthesized WOx/ZrO2 Catalysts. Catalysts, 2018, 8, 292.	1.6	21
184	Favoring the Growth of High-Quality, Three-Dimensional Supercrystals of Nanocrystals. Journal of Physical Chemistry C, 2020, 124, 11256-11264.	1.5	21
185	Far-Infrared Absorption of PbSe Nanorods. Nano Letters, 2011, 11, 2786-2790.	4.5	20
186	Engineering uniform nanocrystals: Mechanism of formation and selfâ€assembly into bimetallic nanocrystal superlattices. AICHE Journal, 2016, 62, 392-398.	1.8	20
187	Charge Transport Modulation in PbSe Nanocrystal Solids by Au _{<i>x</i>} Ag _{1–<i>x</i>} Nanoparticle Doping. ACS Nano, 2018, 12, 9091-9100.	7.3	20
188	Chemo- and Thermomechanically Configurable 3D Optical Metamaterials Constructed from Colloidal Nanocrystal Assemblies. ACS Nano, 2020, 14, 1427-1435.	7.3	20
189	X-ray Mapping of Nanoparticle Superlattice Thin Films. ACS Nano, 2014, 8, 12843-12850.	7.3	19
190	Ligand Coupling Symmetry Correlates with Thermopower Enhancement in Small-Molecule/Nanocrystal Hybrid Materials. ACS Nano, 2014, 8, 10528-10536.	7.3	19
191	Directional Carrier Transfer in Strongly Coupled Binary Nanocrystal Superlattice Films Formed by Assembly and <i>in Situ</i> Ligand Exchange at a Liquid–Air Interface. Journal of Physical Chemistry C, 2017, 121, 4146-4157.	1.5	19
192	Anisotropic nanocrystal shape and ligand design for co-assembly. Science Advances, 2021, 7, .	4.7	19
193	The effects of inorganic surface treatments on photogenerated carrier mobility and lifetime in PbSe quantum dot thin films. Chemical Physics, 2016, 471, 81-88.	0.9	18
194	Anisotropic Cracking of Nanocrystal Superlattices. Nano Letters, 2017, 17, 6501-6506.	4.5	18
195	Coating Evaluation and Purification of Monodisperse, Water-Soluble, Magnetic Nanoparticles Using Sucrose Density Gradient Ultracentrifugation. Chemistry of Materials, 2012, 24, 4008-4010.	3.2	17
196	Statistical Description of CdSe/CdS Dot-in-Rod Heterostructures Using Scanning Transmission Electron Microscopy. Chemistry of Materials, 2016, 28, 3345-3351.	3.2	17
197	Dendronization-induced phase-transfer, stabilization and self-assembly of large colloidal Au nanoparticles. Nanoscale, 2016, 8, 13192-13198.	2.8	17
198	Thermal and Photochemical Reactions of Methanol, Acetaldehyde, and Acetic Acid on Brookite TiO ₂ Nanorods. Journal of Physical Chemistry C, 2017, 121, 11488-11498.	1.5	17

#	Article	IF	CITATIONS
199	Enhanced Carrier Transport in Strongly Coupled, Epitaxially Fused CdSe Nanocrystal Solids. Nano Letters, 2021, 21, 3318-3324.	4.5	17
200	Structural and Valence State Modification of Cobalt in CoPt Nanocatalysts in Redox Conditions. ACS Nano, 2021, 15, 20619-20632.	7.3	17
201	Ultrafast Electron Trapping in Ligand-Exchanged Quantum Dot Assemblies. ACS Nano, 2015, 9, 1440-1447.	7.3	15
202	NeutrAvidin Functionalization of CdSe/CdS Quantum Nanorods and Quantification of Biotin Binding Sites using Biotin-4-Fluorescein Fluorescence Quenching. Bioconjugate Chemistry, 2016, 27, 562-568.	1.8	15
203	3D Nanofabrication via Chemoâ€Mechanical Transformation of Nanocrystal/Bulk Heterostructures. Advanced Materials, 2018, 30, e1800233.	11.1	15
204	Synthesis and Optical Characterization of Polydiacetylenes Containing Carboxylic Acid, Carbamate, Phosphonium, and Quaternary Ammonium Functionalities. Macromolecules, 1996, 29, 6365-6370.	2.2	14
205	Au@TiO2 Core–Shell Nanostructures with High Thermal Stability. Catalysis Letters, 2014, 144, 1939-1945.	1.4	14
206	Structure determination and modeling of monoclinic trioctylphosphine oxide. Acta Crystallographica Section C, Structural Chemistry, 2015, 71, 239-241.	0.2	14
207	Experiments and Simulations Probing Local Domain Bulge and String Assembly of Aligned Nanoplates in a Lamellar Diblock Copolymer. Macromolecules, 2019, 52, 8989-8999.	2.2	14
208	Dynamical Change of Valence States and Structure in NiCu ₃ Nanoparticles during Redox Cycling. Journal of Physical Chemistry C, 2022, 126, 1991-2002.	1.5	14
209	Alternate current magnetic property characterization of nonstoichiometric zinc ferrite nanocrystals for inductor fabrication via a solution based process. Journal of Applied Physics, 2016, 119, .	1.1	13
210	Synthesis and Characterization of Core-Shell Cu-Ru, Cu-Rh, and Cu-Ir Nanoparticles. Journal of the American Chemical Society, 2022, 144, 7919-7928.	6.6	13
211	Nanoparticle diffusion during gelation of tetra poly(ethylene glycol) provides insight into nanoscale structural evolution. Soft Matter, 2020, 16, 2256-2265.	1.2	12
212	Quantitative 3D real-space analysis of Laves phase supraparticles. Nature Communications, 2021, 12, 3980.	5.8	12
213	Grafted Nanoparticle Surface Wetting during Phase Separation in Polymer Nanocomposite Films. ACS Applied Materials & Interfaces, 2021, 13, 37628-37637.	4.0	12
214	Dynamic magnetic field alignment and polarized emission of semiconductor nanoplatelets in a liquid crystal polymer. Nature Communications, 2022, 13, 2507.	5.8	12
215	<i>In Situ</i> EXAFS-Based Nanothermometry of Heterodimer Nanocrystals under Induction Heating. Journal of Physical Chemistry C, 2022, 126, 3623-3634.	1.5	11
216	Synthesis and nonlinear optical properties of functionalised polydiacetylenes and their complexes with transition metals. Journal of Materials Chemistry, 1999, 9, 1251-1256.	6.7	10

#	Article	IF	CITATIONS
217	Nanorod Mobility Influences Polymer Diffusion in Polymer Nanocomposites. ACS Macro Letters, 2017, 6, 869-874.	2.3	10
218	Distinguishing Electron and Hole Dynamics in Functionalized CdSe/CdS Core/Shell Quantum Dots Using Complementary Ultrafast Spectroscopies and Kinetic Modeling. Journal of Physical Chemistry C, 2021, 125, 31-41.	1.5	10
219	The dendritic effect and magnetic permeability in dendron coated nickel and manganese zinc ferrite nanoparticles. Nanoscale, 2017, 9, 13922-13928.	2.8	9
220	Spectroscopic characterization of a highly selective NiCu ₃ /C hydrodeoxygenation catalyst. Catalysis Science and Technology, 2018, 8, 6100-6108.	2.1	9
221	Nanorod position and orientation in vertical cylinder block copolymer films. Soft Matter, 2020, 16, 3005-3014.	1.2	9
222	Efficient photoluminescence of isotropic rare-earth oxychloride nanocrystals from a solvothermal route. Chemical Communications, 2020, 56, 3429-3432.	2.2	9
223	Broadband Circular Polarizers via Coupling in 3D Plasmonic Meta-Atom Arrays. ACS Photonics, 2021, 8, 1286-1292.	3.2	9
224	Monodisperse Nanocrystal Superparticles through a Source–Sink Emulsion System. Chemistry of Materials, 2022, 34, 2779-2789.	3.2	9
225	A comparison of hierarchical Pt@CeO2/Si–Al2O3 and Pd@CeO2/Si–Al2O3. Catalysis Today, 2015, 253, 137-141.	2.2	7
226	The Influence of Surface Platinum Deposits on the Photocatalytic Activity of Anatase TiO ₂ Nanocrystals. Journal of Physical Chemistry C, 2019, 123, 10477-10486.	1.5	7
227	Plasmonic Elastic Capsules as Colorimetric Reversible pHâ€Microsensors. Small, 2020, 16, 1903897.	5.2	7
228	Nanocrystal Superparticles with Whispering-Gallery Modes Tunable through Chemical and Optical Triggers. Nano Letters, 2022, 22, 4765-4773.	4.5	7
229	Evaporation-Driven Coassembly of Hierarchical, Multicomponent Networks. ACS Nano, 2022, 16, 4508-4516.	7.3	6
230	A semi-combinatorial approach for investigating polycatenar ligand-controlled synthesis of rare-earth fluoride nanocrystals. Nanoscale, 2017, 9, 8107-8112.	2.8	5
231	Morphological Dependence of the Thermal and Photochemical Reactions of Acetaldehyde on Anatase TiO2 Nanocrystals. Topics in Catalysis, 2018, 61, 365-378.	1.3	5
232	Tunable Plasmonic Microcapsules with Embedded Noble Metal Nanoparticles for Optical Microsensing. ACS Applied Nano Materials, 2022, 5, 2828-2838.	2.4	5
233	Impurities in Nanocrystal Thin-Film Transistors Fabricated by Cation Exchange. Journal of Physical Chemistry Letters, 2021, 12, 6514-6518.	2.1	4
234	Electron accepting naphthalene bisimide ligand architectures for modulation of π–π stacking in nanocrystal hybrid materials. Nanoscale Horizons, 2020, 5, 1509-1514.	4.1	3

#	Article	IF	CITATIONS
235	Engineering the composition of bimetallic nanocrystals to improve hydrodeoxygenation selectivity for 2-acetylfuran. Applied Catalysis A: General, 2020, 606, 117808.	2.2	2
236	Electrochemically deposited molybdenum disulfide surfaces enable polymer adsorption studies using quartz crystal microbalance with dissipation monitoring (QCM-D). Journal of Colloid and Interface Science, 2022, 614, 522-531.	5.0	2
237	Effect of Graft Length and Matrix Molecular Weight on String Assembly of Aligned Nanoplates in a Lamellar Diblock Copolymer. Macromolecules, 2022, 55, 3166-3175.	2.2	2
238	Simultaneous Position and Orientation Imaging of Polarized Fluorescence from Rod-In-Rod Semiconductor Nanoparticles on Cytoplasmic Dynein. Biophysical Journal, 2014, 106, 197a.	0.2	0
239	In-situ Study of Coarsening Mechanisms of Supported Metal Particles in Reducing Gas. Microscopy and Microanalysis, 2015, 21, 643-644.	0.2	0
240	Unraveling the Self-Assembly Pathway of Binary Nanocrystal Superlattices. , 0, , .		0
241	In-line Production of Colloidal Microlasers. , 0, , .		Ο